

The mass-to-distance ratio for a set of megamaser AGN black holes by employing a general relativistic method

A. González-Juárez,¹ M. Momennia,^{1,2} A. Villalobos-Ramírez,¹ and A. Herrera-Aguilar^{1,*}

¹ Instituto de Física Luis Rivera Terrazas (IFUAP), Benemérita Universidad Autónoma de Puebla, Puebla 72570, México

² Instituto de Física y Matemáticas, Universidad Michoacana de San Nicolás de Hidalgo, Michoacán 58040, México

Received Month XX, XXXX; accepted Month XX, XXXX

ABSTRACT

Context. Motivated by recent achievements of a full general relativistic method in determining black hole (BH) parameters, we continue to estimate the mass-to-distance ratio of the supermassive BHs hosted at the core of the active galactic nuclei (AGNs) of NGC 1320, NGC 1194, NGC 5495, and Mrk 1029.

Aims. To study the properties of SMBHs at the centers of selected AGNs by a full general relativistic method which allows us to address the potential detection of relativistic effects within such astrophysical systems.

Methods. In order to perform statistical estimations with publicly available observational data, we use a general relativistic model that describes black hole rotation curves and further employ a Bayesian fitting method.

Results. We estimate the mass-to-distance ratio of the aforementioned BHs, their x_0 -offset as well as the recessional redshifts of the host galaxies produced by both peculiar motion and cosmological expansion of the Universe. Finally, we calculate the gravitational redshift of the closest maser to the BH for each AGN. This gravitational redshift is a general relativistic effect produced by the gravitational field of the BH properly included in the modeling.

Key words. black hole physics – masers – galaxies: nuclei – galaxies: high-redshift – methods: statistical.

1. Introduction

Nowadays, one of the most active research areas in modern astrophysics is to search for observational evidence to support the existence of BHs in nature. Although BHs first have been found as mathematical solutions to Einstein field equations, several phenomena could potentially lead to the formation of a BH. As the most promising scenarios, we can refer to the collapse of a massive star to form a stellar-mass BH, processes in galactic dynamics to create supermassive black holes (SMBHs) in the center of most galaxies (Kormendy & Richstone 1995), and fluctuations in the early universe that could generate primordial BHs.

The discovery of quasars and AGNs gave rise to the idea that SMBHs are located at the core of many galaxies. The reason is that only SMBHs can compellingly explain the production of huge rates of luminous radiation within small compact volumes. A viable explanation of this phenomenon is the conversion of the gravitational energy into radiation in their potential well, rendering a long-term stable central mass (see, for instance, Celotti et al. (1999) and references therein). The tighter constraint on the compactness of the central object comes from the highly energetic X-ray radiation. This electromagnetic radiation, along with other spectral information like line emission from gas particles with velocities up to thousands of km s^{-1} , can be satisfactorily explained by the presence of a central SMBH in these galaxies.

In the past decades, two groups of astronomers (the Galactic Center teams at MPE and UCLA) have been tracking the orbital motion of a set of stars around the gravitational center of our Galaxy (Genzel & Townes 1987; Genzel et al. 1996; Ghez et al.

1998). The detected velocities and accelerations of these stars provided strong evidence for the existence of a central source, called Sagittarius A* (Sgr A*), to be a SMBH with mass of $\approx 4.0 \times 10^6 M_\odot$ (Do et al. 2019; Gravity Collaboration et al. 2019, 2020). In these works the putative BH mass in the center of the Milky Way has been estimated based on Newtonian models with relativistic corrections.

Furthermore, the two SMBHs at the core of M87 and the Milky Way galaxies have been studied by the Event Horizon Telescope (EHT) Collaboration with the aim to capture their shadow image. In this regard, the EHT revealed the first images of the shadows of these SMBHs (Event Horizon Telescope Collaboration et al. 2019, 2022a, 2022b), hence investigating this phenomenon attracted much attention recently.

However, it is worth noting that in order to study the putative SMBHs, some of the various aforementioned AGNs, a full general relativistic method was lacking and this shows the importance of the present study. This relativistic method allows us to address the potential detection of relativistic effects within such astrophysical systems.

The Megamaser Cosmology Project¹ (MCP) of the National Radio Astronomy Observatory is a collaboration with the Cosmic Microwave Background project from Wilkinson Microwave Anisotropy Probe and Planck missions. The primary aim of the MCP is to determine the Hubble Constant from galaxies in the Hubble flow whose discs contain water megamasers, Reid et al.

¹ <https://safe.nrao.edu/wiki/bin/view/Main/MegamaserCosmologyProject>

* Just to show the usage of the elements in the author field

(2009). Moreover, they also estimate the distance to these galaxies and the BH mass hosted in their center.

Water megamasers are water vapor clouds in AGNs emitting at 22 GHz by stimulated emission, moving in nearly circular orbits, and forming thin disc structures mostly observable (almost) edge-on. In the MCP, the authors have used Keplerian motion with relativistic corrections to fit the trajectories of the masers in the BH accretion discs for 24 different galaxies reported in Reid et al. (2009); Kuo et al. (2011); Kuo et al. (2013); Gao et al. (2016), Zhao et al. (2018); Kuo et al. (2020).

On the other hand, a general relativistic method has been implemented to estimate the mass-to-distance ratio M/D (D is the distance from the observer to the BH) of the BH hosted at the core of NGC 4258 in Nucamendi et al. (2021). This relativistic model takes into account a system of probe particles that circularly orbit a Schwarzschild BH in the equatorial plane. In this scenario, the required observational quantities to perform the estimations are the frequency shifts experienced by the photons emitted by test particles (in this case, by the megamasers) and their positions (see Herrera-Aguilar & Nucamendi (2015) and Banerjee et al. (2022) for the full description of a rotating BH model). Thus, as a result, in Nucamendi et al. (2021) the M/D ratio of the SMBH of NGC 4258 was estimated to be $M/D = (0.5326 \pm 0.0002) \times 10^7 M_\odot \text{ Mpc}^{-1}$. Also, the authors provided the computation of general and special relativistic effects: The gravitational redshift produced by the BH mass and the special relativistic boost that mimics the peculiar motion of the host galaxy from Earth.

As another application of this general relativistic model, we can refer to (Villalobos-Ramírez et al. 2022) where the M/D ratio of the galaxy TXS-2226-184 was estimated for the first time. Furthermore, the authors have quantified the BH mass by using the distance reported in Surcis et al. 2020 and found that the result is compatible with the mass obtained from the mass-luminosity correlation. By comparing both BH mass results, the accuracy of the general relativistic model is one order of magnitude better than that of the mass-luminosity correlation.

More recently, the M/D ratio has been estimated for ten more galaxies of the MCP systems in Villaraos et al. (2022). In these water megamaser systems, it is possible to identify three groups: The first group represents frequency shifted photons close to the systemic redshift of the host galaxy, whereas the other two groups are highly frequency-shifted photons coming from the megamasers at the points of maximum emission. They have found that the velocity corresponding to the gravitational redshift of the closest maser to each BH is about $1 - 6 \text{ km s}^{-1}$ and BH masses range from 10^6 to $10^7 M_\odot$, a mass domain associated with supermassive BHs.

In the present study, we apply the general relativistic method and a Bayesian statistical treatment to investigate four more megamaser systems among the remaining 14 MCP galaxies. For NGC 1320, we estimated four parameters including the M/D ratio, x -offset, and y -offset of the BH as well as the recession velocity v_{rec} . Moreover, we estimate the three parameters including M/D ratio, x -offset, and v_{rec} , for the galaxies NGC 1194, NGC 5495, and Mrk 1029. We did not fit the rest of the galaxies because of some particular features they display. For example, the case of J1346+5228 has a few reported masers, just one redshifted and one blueshifted masers, leading to poor statistical results. AGNs of NGC 2824 and J0350-0127 are reported without redshifted and blueshifted masers, and because the model is based on these observations, we could not perform an estimation. Observations of NGC 6926 show an extra group of redshifted megamasers whose treatment goes out of the scope of this work.

Finally, UGC 6093 and Mrk 1 are two galaxies that have been reported with position uncertainties of the same order that those of their angular distance which led to imprecise results.

We organize this paper as follows: In the next section, we briefly review the general relativistic model implemented in this work. In Sec. 3, the Bayesian approach applied to the model of section 2 is exposed and the results of the statistical fit are presented. Finally, we discuss the results in Sec. 4.

2. General Relativistic Model

This model is based on a general relativistic formalism that has been developed in (Herrera-Aguilar & Nucamendi 2015) and (Banerjee et al. 2022) to analytically express the mass and spin parameters of the rotating Kerr BH in terms of observational redshift/blueshift of photons emitted by massive particles orbiting the BH and their orbital parameters. This scenario has been employed in Nucamendi et al. (2021) for a static and spherically symmetric Schwarzschild BH of the form

$$ds^2 = \frac{dr^2}{f} + r^2(d\theta^2 + \sin^2\theta d\varphi^2) - f dt^2, \quad f = 1 - \frac{2m}{r}, \quad (1)$$

where m is the total mass of the BH in $G = 1 = c$ units. As the test particles of the model, we have water megamasers orbiting circularly a central static BH of the AGN accretion disc characterized by the line element (1). These megamasers are distributed on the entire disc and are stimulated by the BH, making them to emit photons. Then, we are able to observe the shift in their frequency at certain positions of the orbit. In this context, the total frequency shift of the photons is given by

$$1 + z_{tot1,2} = (1 + z_{Schw1,2})(1 + z_{rec}), \quad (2)$$

where z_{rec} is the recessional redshift composed by (Davis & Scrimgeour 2014)

$$1 + z_{rec} = (1 + z_{cosm})(1 + z_{boost}), \quad 1 + z_{boost} = \frac{1 + \beta}{\sqrt{1 - \beta^2}}, \quad (3)$$

In this relation, z_{cosm} is the cosmological redshift, z_{boost} is the frequency shift generated by a special relativistic boost that depends on the peculiar velocity v_p characterizing the radial motion of the galaxy (Rindler 1982) and $\beta = v_p/c$. We define the peculiar velocity in terms of the peculiar redshift as $v_p = c z_p$. Besides, the Schwarzschild frequency shift consists of the kinematic redshift/blueshift and the gravitational redshift as

$$1 + z_{Schw1,2} = 1 + z_{grav} + z_{kin\pm}, \quad (4)$$

in which z_{grav} is the gravitational redshift due to the spacetime curvature generated by the BH mass, and $z_{kin\pm}$ is the kinematic redshift/blueshift originated by the frequency shift of photons emitted by moving masers, i.e. the local Doppler effect, with the following explicit forms

$$z_{grav} = \sqrt{\frac{1}{1 - 3\frac{m}{r_e}}} - 1, \quad z_{kin\pm} = \pm \sqrt{\frac{\frac{m}{r_e}}{(1 - 3\frac{m}{r_e})(1 - 2\frac{m}{r_e})}}, \quad (5)$$

where r_e is the emitter radius (the radius of megamaser features in this case). We use the approximation $\Theta \approx r_e/D$, where Θ is the angular distance between a given maser and the BH in our model and estimations.

3. Statistical fit

In this paper, we apply a Bayesian statistical treatment to observational data based on the Monte Carlo method that uses Markov

Table 1. Reported parameters of the sample galaxies. Column 1: Name of the source. Column 2: Source position (J2000). Column 3: Fitted mass of the SMBHs. Column 4: Estimated distance to the sources. Column 5: Computed M/D ratio from columns 3 and 4. Column 6: Fitted recession velocities. Column 7: Reported inclination angle θ_0 for NGC 1194, NGC 5495 and Mrk 1029, and fixed inclination angle for NGC 1320.

Source	Position R.A. (h : m : s) Decl. ($^\circ$: $'$: $''$)	Mass ($10^7 M_\odot$)	Distance (Mpc)	M/D ($10^5 M_\odot$)/Mpc	Recession velocity (km/s)	Inclination angle ($^\circ$)	Reference
NGC 1194	03:03:49.10864 -01:06:13.4743	6.5 ± 0.3	$55.4 \pm 3.9^*$	11.733	4051 ± 15	85^a	Kuo et al. (2011)
NGC 5495	14:12:23.35 -27:06:29.20	1.1 ± 0.2	95.7 ± 5.3	1.149	6839.6 ± 67.0	95 ± 1^b	Gao et al. (2016)
Mrk 1029	02:17:03.566 05:17:31.43	0.19 ± 0.05	120.8 ± 6.6	0.158	9129.9 ± 26.0	79 ± 2^b	Gao et al. (2016)
NGC 1320	03:24:48.70 -03:02:32.30	0.55 ± 0.25	34.2 ± 1.9	1.608	2829.2 ± 11.4	90^c	Gao et al. (2016)

NOTES.

Label a represents values reported without uncertainty.

Label b refers to the inclination angle fixed through observations of systemic masers in Gao et al. (2016).

Label c refers to the fixed inclination angle due to the absence of systemic maser features in Gao et al. (2016).

Label d refers to the inclination angle fixed through observations of systemic masers in Zhao et al. (2018).

Label * indicates the distance to NGC 1194 estimated in Kamali et al. (2017).

chains. This treatment consists of a least squares χ^2 fit of the M/D ratio, z_{rec} and the displacement of both x - and y -offsets of the central object which is given by

$$\chi^2 = \sum_{k=1} \frac{[z_{k,obs} - (1 + z_{grav} + \epsilon \sin \theta_0 z_{kin\pm})(1 + z_{rec}) + 1]^2}{\sigma_{z_{tot1,2}}^2 + \kappa^2 \epsilon^2 z_{kin\pm}^2 \sin^2 \theta_0 (1 + z_{rec})^2}, \quad (6)$$

where $\sigma_{z_{tot1,2}} = |\delta z_{tot1,2}|$ is the variation of total redshift, θ_0 is the inclination angle, and the quantities ϵ and κ refer to the spread of the maser features on the azimuth angle (Herrnstein et al. 2005)

$$\epsilon \approx 1 - \frac{\delta\varphi^2}{2} + \frac{\delta\varphi^4}{24}, \quad \kappa^2 \approx \frac{\delta\varphi^4}{4}. \quad (7)$$

Here, the first expansion corresponds to the cosine function of φ and κ denotes the induced uncertainties of the maser scattering under the assumptions $\varphi \ll 1$ and $\varphi \sim \delta\varphi$. In addition, $\sigma_{z_{tot1,2}}^2$ in the χ^2 relation (6) represents the error of the total redshift with the following explicit form

$$\delta z_{tot1,2} = (\delta z_{grav} + \delta z_{kin\pm})(1 + z_{rec}), \quad (8)$$

where

$$\delta z_{grav} = (1 + z_{grav})^3 \left(\frac{-3m}{2r_e^2} \right) \delta r_e, \quad (9)$$

$$\delta z_{kin\pm} = \epsilon \sin \theta_0 (z_{kin\pm})^3 \left(\frac{6m^2 - r_e^2}{2mr_e^2} \right) \delta r_e, \quad (10)$$

$$\delta r_e = \sqrt{\left(\frac{x_i - x_0}{r} \right)^2 \delta_x^2 + \left(\frac{y_i - y_0}{r} \right)^2 \delta_y^2}, \quad (11)$$

such that (x_i, y_i) is the position of the i -th megamaser on the sky, $\{\delta_x, \delta_y\}$ are their respective errors, and (x_0, y_0) represents the BH position.

3.1. Parameter fitting: priors and posteriors

The convention used by MCP to allocate the origin of their reference systems at some position of the masers is to consider the brightest maser. In this paper, although we used the database of (Kuo et al. (2011) and Gao et al. (2016)), we employed a rotated distribution of the masers to the horizontal axis. We apply this rotation by considering the reported position angle (P.A.) for the megamaser systems.

This statistical fit takes into account the positions in the plane perpendicular to the line of sight (LOS) of the water masers with their respective uncertainties in the positions and the frequency shift of the photons emitted by these masers.

The BH parameters undergoing the Bayesian statistical fit are the mass-to-distance ratio M/D , the recessional redshift z_{rec} as well as the horizontal offset x_0 and the vertical offset y_0 of the BH position. However, due to the characteristics of the masers distribution of individual galaxies, the model does not render the estimations of all the parameters for each case. For instance, for most of the fitted galaxies, the parameter y_0 cannot be estimated due to the thin character of the disc.

Then, for the galaxies NGC 1194, Mrk 1029 and NGC 1320, we fix the scattering angle of maser features $\delta\varphi$ to obtain the reduced χ_{red}^2 value close to unity. For NGC 5495, the χ_{red}^2 value is less than one. In this case, the maser position errors are much larger than those shown in the rest of galaxies under consideration (see Table 2 and corresponding Fig. 1).

Finally, we calculate the gravitational redshift of the closest maser to the BH for these galaxies and present results in Table 3. We consider the contribution of this gravitational redshift in our estimations, an effect that has been properly included in our general relativistic study.

3.1.1. NGC 1194

NGC 1194 is a system with three groups of maser features (see Fig. 1) and the information of this maser system is consistent with a thin disc that is distributed in the sky with a P.A. of approximately 157° . We perform the statistical fit to the mass-to-distance ratio, the recessional redshift, and the BH x -

Table 2. Posterior parameters. Column 1: Name of the source. Column 2: Fitted mass-to-distance ratio. Column 3: Horizontal offset (x_0) of the BH found by the Bayesian fit. Column 4: Vertical offset (y_0) of the BH either found by the Bayesian fit or fixed. Column 5: Recessional redshift found by the fit. Column 6: Recession velocity after the optical definition of the redshift. Column 7: Scattering in the azimuth angle. Column 8: Reduced χ^2 of the best fit.

Source	M/D ($10^5 M_\odot/\text{Mpc}$)	x_0 (mas)	y_0 (mas)	z_{rec} (10^{-2})	v_{rec} (km/s)	$\delta\varphi$ ($^\circ$)	χ^2_{red}
NGC 1194	$13.100^{+0.211}_{-0.209}$	$0.379^{+0.133}_{-0.131}$	0.0*	1.363 ± 0.004	$4085.984^{+12.527}_{-12.421}$	11	1.206
NGC 5495	$1.153^{+0.208}_{-0.174}$	$-0.071^{+0.174}_{-0.118}$	0.0*	$2.281^{+0.018}_{-0.019}$	$6839.055^{+53.393}_{-57.772}$	0	0.282
Mrk 1029	0.144 ± 0.011	$-0.376^{+0.143}_{-0.138}$	0.0*	3.035 ± 0.004	$9099.332^{+12.710}_{-11.252}$	14	1.385
NGC 1320	$1.497^{+0.071}_{-0.069}$	$-1.243^{+0.147}_{-0.132}$	$-0.761^{+0.149}_{-0.142}$	0.942 ± 0.002	$2825.433^{+6.158}_{-6.389}$	17	1.127

NOTE: The double horizontal line separates different galaxies according to the number of estimated parameters.

We estimate 3 parameters for the first three galaxies and 4 parameters for the fourth galaxy.

The label * indicates that we fixed this parameter.

offset, while we fix its y -offset aligned with the redshifted and blueshifted masers. The estimated $M/D = (1.31 \pm 0.02) \times 10^6 M_\odot/\text{Mpc}$ implies $M = (7.26 \pm 0.52) \times 10^7 M_\odot$ for the BH mass when taking into account the distance reported in Table 1. Besides, by considering the v_{rec} estimation of the general relativistic approach and the reported recession velocity in Kuo et al. (2011) (see Table 1), we find that these results exclude each other. It is worth mentioning that since the general relativistic model employed in this paper is different from prior works, the source of this disagreement and getting different results is due to the difference in the modeling. The scattering angle $\delta\varphi = 11^\circ$ renders $\chi^2_{red} = 1.206$.

3.1.2. NGC 5495

NGC 5495 is a Seyfert 2 AGN-type galaxy with an original north-south orientation maser disc with a P.A. of $176^\circ \pm 5^\circ$. For this galaxy, we estimate the three parameters: the ratio $M/D = 1.15^{+0.21}_{-0.17} \times 10^5 M_\odot/\text{Mpc}$ that implies a BH mass of $M = 1.10^{+0.21}_{-0.18} \times 10^7 M_\odot$, the recession velocity v_{rec} , and the BH x -offset, fitted without a scattering angle leading to reduced $\chi^2_{red} = 0.28$. The resulting BH position is optimal in the sense that the statistical fit renders it just behind the systemic masers (see Fig. 1). For this maser distribution, a 5° error in the P.A. has been reported (Gao et al. 2016). By propagating the error in the position angle during rotation, we obtain a 0.16% change in the estimated M/D ratio.

3.1.3. Mrk 1029

Mrk 1029 is a galaxy with an original linear maser distribution from the north-east to the south-west at a P.A. of $218^\circ \pm 10^\circ$. As the first step to analyzing this system and extracting some information, we follow the MCP and consider a disk consisting of particles in a circular motion. Indeed, since our goal in this work is to investigate the general relativistic effects and quantify the gravitational redshift, we keep the geometry of the disk as in the previous study (Gao et al. 2016). For this galaxy, we estimate three parameters, namely, the ratio $M/D = (1.44 \pm 0.11) \times 10^4 M_\odot/\text{Mpc}$ that implies a BH mass $M = (1.74 \pm 0.16) \times 10^6 M_\odot$, the recession velocity v_{rec} , and the x -offset of BH position. These parameters have been fitted for a scattering angle of $\delta\varphi = 14^\circ$

and led to a reduced $\chi^2_{red} = 1.385$. For this galaxy, the recession velocities $9076 \pm 32 \text{ km s}^{-1}$ and $9160 \pm 61 \text{ km s}^{-1}$, reported in (Huchra et al. 1999; De Vaucouleurs et al. 1991), respectively, are compatible with our estimated value $9099.33^{+12.71}_{-11.25} \text{ km s}^{-1}$ (see Table 2). Again, the resulting BH position is optimal in the sense that the fit yields its location among the systemic masers.

On the other hand, by propagating the P.A. error during the rotation of the maser system, the M/D estimation changes about 1.19%, a quantity that is within its error (see Table 2). Hence, we can neglect the error associated with the P.A.

3.1.4. NGC 1320

The masers of NGC 1320 have been found in just two distinct frequency shifted groups. The maser distribution shows an east-west orientation with a P.A. of $75^\circ \pm 10^\circ$. By considering our results, we could not recognize any systemic maser feature because there are no masers with a speed near the recession velocity of 2825 km s^{-1} . For this system we estimated 4 parameters: The BH x - and y -offsets, the recession velocity and the mass-to-distance ratio $M/D = 1.50 \pm 0.07 \times 10^5 M_\odot/\text{Mpc}$. In this case, the corresponding BH mass reads $M = (5.12 \pm 0.37) \times 10^6 M_\odot$. By considering $\delta\varphi = 17^\circ$, the model gives a reduced $\chi^2_{red} = 1.127$.

With this general relativistic model, the x -offset of the BH led to a position very close to the blueshifted maser group. In addition, by considering the propagation of the P.A. error under the rotation, we get a slight difference of 2.64% in the estimation of the M/D ratio. Despite being the galaxy with the biggest change in the mass-to-distance ratio, it is still within the M/D error, as we can see from Table 2.

4. Discussion and conclusions

Here, the four AGNs NGC 1194, UGC 5495, Mrk 1029, and NGC1320 from the MCP have been studied in order to fit the M/D ratio of the central BH hosted at their core, along with other parameters like the recession velocity and the BH x - and/or y -offset.

It is worth mentioning that, in this paper, we estimated the M/D ratio of several BHs by using a general relativistic method. Our results are different from the MCP ones where the corresponding BH masses have been estimated through a Newton-

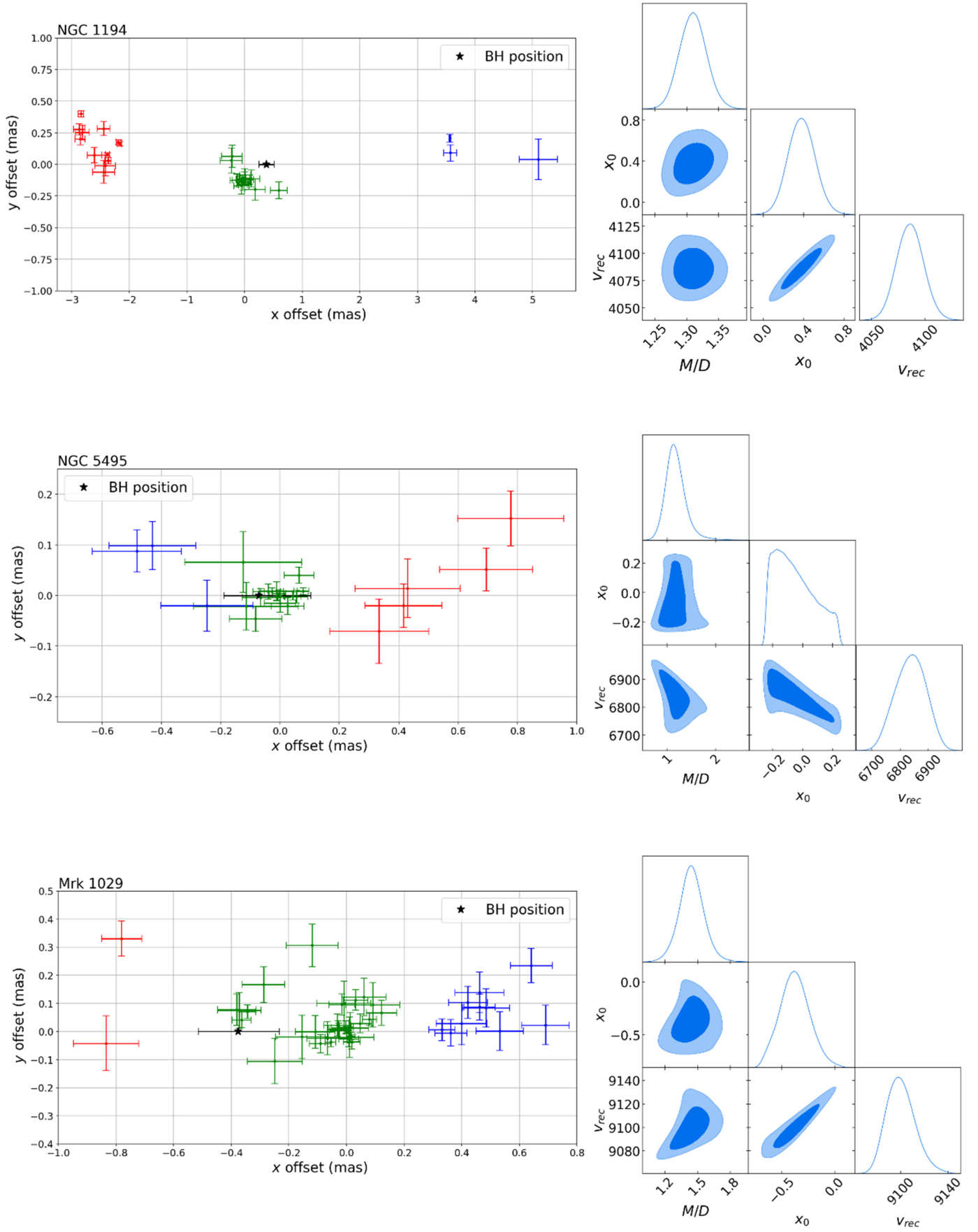


Fig. 1. Maser discs and posterior probability distributions for the galaxies NGC 1194, NGC 5495, and Mrk 1029. The maser disc plots show the three groups of maser features viewed edge-on with their observational error. The star symbol refers to the best fit for the BH position on the disc. The black line through this star symbol indicates the uncertainty in the position of BH. The blue graphs in the right panels show the posterior probability distribution with the contour levels corresponding to 1σ and 2σ confidence regions.

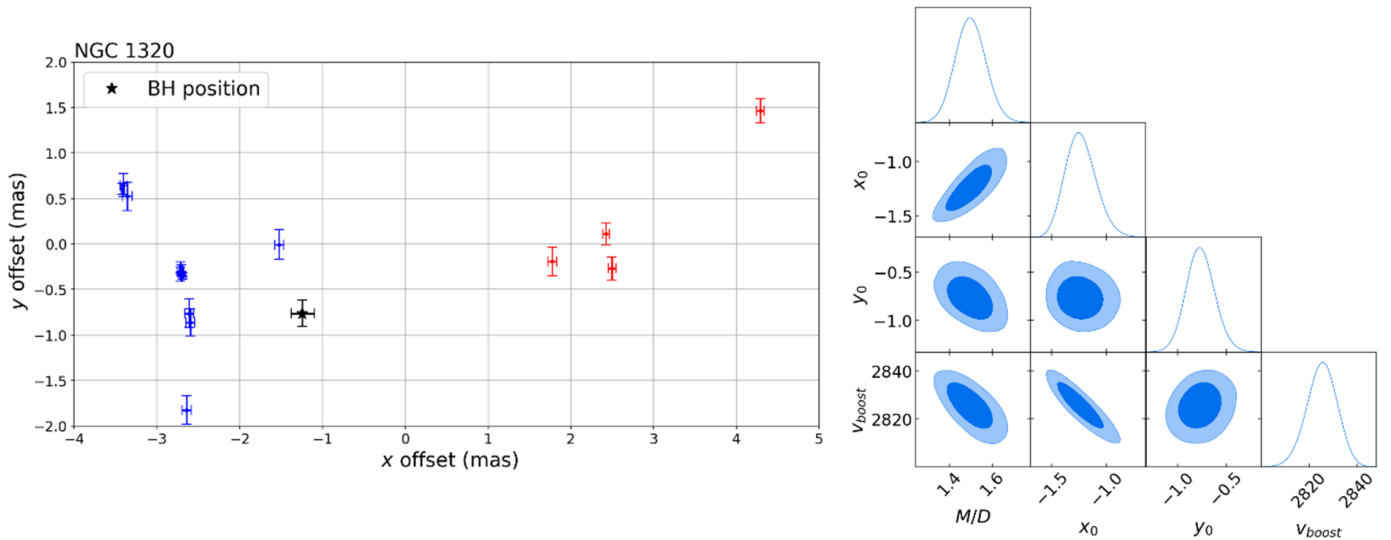


Fig. 2. Maser disc and posterior probability distribution for the galaxy NGC 1320. The maser disc plot shows an AGN with particular characteristics. NGC 1320 does not have a systemic maser feature group and the model allows estimating 4 parameters. The star symbol in the left panel indicates the best fit for the BH position on the disc and the black line through this symbol denotes the uncertainty in the BH position. The blue graph in the right panel shows the posterior probability distribution with the contour levels corresponding to 1σ and 2σ confidence regions.

Table 3. The gravitational redshift of the closest maser to the BH.

Source	Maser feature	Distance to the closest maser (mas)	Gravitational redshift (10^{-6})	Associated velocity (km/s)
NGC 1194	Red	2.549	7.610	2.282
NGC 5495	Blue	0.189	9.036	2.709
Mrk 1029	Red	0.460	0.465	0.139
NGC 1320	Blue	0.809	2.740	0.821

nian approach with relativistic corrections. Therefore, we cannot compare both results directly since different quantities are estimated. Notwithstanding, we are currently developing a method to decouple M and D so that the results of both approaches can be directly confronted in the near future.

In addition, we have observed that, in general, the recession velocities of these galaxies are compatible with the corresponding estimations reported in Table 1, except for NGC 1194. For this galaxy the recession velocities yielded by both fits exclude each other. Besides, the recession velocity of the galaxy NGC 1194 has been estimated by using an optical spectral line fit and the HI continuum in (Pesce et al. 2018).

On the other hand, the general relativistic formalism, that we have employed to estimate the BH parameters, allows us to quantify the gravitational redshift of each highly frequency-shifted maser. In this regard, we have calculated the gravitational redshift of the closest maser to each SMBH, and the results are presented in Table 3.

Moreover, in order to compare the M/D ratio presented in this study with the MCP estimations of BH mass, we calculated the mass-to-distance ratio using the MCP results by dividing the mass over the distance (see Column 5 of Table 1). Note that we did not propagate the mass and distance uncertainties in M/D ratio since the uncertainty in the mass-to-distance ratio of the MCP results inherits the large distance error during propagation, and thus, the resultant uncertainties would be misleading. On

the other hand, we have calculated the BH mass from the M/D estimations multiplied by the distance taken from Table 1 and propagated the corresponding uncertainty for each galaxy.

Finally, we finish our paper with a couple of suggestions for future work. Within this general relativistic model, considering the systemic masers in the statistical fits in order to improve the accuracy of the estimations would be interesting. Besides, it would be nice to break the M/D degeneracy in order to obtain independent estimations for the BH mass and the distance to the BH. These extensions are currently under examination.

Acknowledgements. All authors are grateful to D. Villaraos for shared experience and illuminating discussions about previous work and A. Christen for sharing his expertise on statistical estimations. The authors thank the Megamaser Cosmology Project researchers for making the observational data used in this work publicly available and CONACYT for support under grant No. CF-MG-2558591. A.G.-J. and M.M. thank SNII and were supported by CONACYT through the postdoctoral grants Nos. 446473 and 31155, respectively. A.V.-R. acknowledges financial assistance from CONACYT through grant No. 1007718. A.H.-A. was supported by VIEP-BUAP grant No. 242 as well as by SNII.

Data Availability

The data used in this paper for each AGN are publicly available in the following references: Kuo et al. (2011) (NGC 1194), Gao et al. (2016) (NGC 5495, Mrk 1029, NGC 1320).

References

- Kuo, C. Y., Braatz J. A., Condon, J. J., Impellizzeri, C. M. V., Lo, K. Y., Zaw, I., Schenker, M., Henkel, C., Reid, M. J., Greene, J. E. 2011, *ApJ*, 727, 1
- Reid, M. J., Braatz, J. A., Condon, J. J., Lo, K. Y., Kuo, C. Y., Impellizzeri, C. M. V., Henkel, C. 2013, *ApJ*, 767, 2
- C. Y. Kuo, J. A. Braatz, M. J. Reid, K. Y. Lo, J. J. Condon, C. M. V. Impellizzeri, C. Henkel 2013, *ApJ*, 767, 2
- Kuo, C. Y., Braatz, James, Reid, Mark, Lo, Fred, Condon, James, Impellizzeri, C., Henkel, Christian 2012, *ApJ*, 767
- Kuo, C. Y., Braatz, J., Lo, K., Reid, M., Suyu, S., Pesce, D., Condon, James, Henkel, C., Impellizzeri, C. 2014, *ApJ*, 800
- Gao, F., Braatz, J., Reid, M., Lo, K., Condon, James, Henkel, C., Kuo, Chien-Yin, Impellizzeri, C., Pesce, D., Zhao, W. 2015, *ApJ*, 817
- Gao, F., Braatz, J., Reid, M., Condon, James, Greene, J., Henkel, C., Impellizzeri, C., Lo, K., Kuo, Chien-Yin, Pesce, D., Wagner, J., Zhao, W. 2016, 834
- Zhao, W., Braatz, J., Condon, James, Lo, K., Reid, M., Henkel, C., Pesce, D., Greene, J., Gao, F., Kuo, C. Y., Impellizzeri, C. 2018, *ApJ*, 854
- Pesce, D., Braatz, J., Reid, M., Condon, James, Gao, F., Henkel, C., Kuo, Chien-Yin, Lo, K., Zhao, W. 2020, *ApJ*, 890
- Davis, T. M., Scrimgeour, Morag I. 2014, *MNRAS*, 442, 2
- Abbott, B. P., Abbott, R., Abbott, T. D. et al. 2016, *Phys. Rev. Lett.*, 116, 6
- Genzel, R., Townes, C. H. 1987, *Annu. Rev. Astron. Astrophys.*, 25
- Abbott, B. P., Abbott, R., Abbott, T. D. et al. 2019, *Phys. Rev. X*, 9, 3
- Genzel, R., Thatte, N., Krabbe, A., Kroker, H., Tacconi-Garman, L. E. 1996, *ApJ*, 472
- Ghez, A. M., Klein, B. L., Morris, M., Becklin, E. E. 1998, *ApJ*, 509, 2
- Ghez, A. M., Salim, S., Hornstein, S. D., Tanner, A., Lu, J. R., Morris, M., Becklin, E. E., Duchêne, G. 2005, *ApJ*, 620, 2
- Ghez, A. M., Salim, S., Weinberg, N. N. et al. 2008, *ApJ*, 689, 2
- Claussen, M. J., Lo, K. -Y. 1986, *ApJ*, 308
- Lo, K. Y. 2005, *Annu. Rev. Astron. Astrophys.*, 43, 1
- Churchwell, E., Witzel, A., Huchtmeier, W., Pauliny-Toth, I., Roland, J., Sieber, W. 1977, *Astron. Astrophys.*, 54
- Gravity Collaboration et al. 2020, *Astron. Astrophys.*, 636
- Gravity Collaboration et al. 2018, *Astron. Astrophys.*, 615
- Miyoshi, M., Moran, J., Herrnstein, J., Greenhill, L. Nakai, N., Diamond, P., Inoue, M. 1995, *Nature*, 373
- Herrnstein, J. R., Moran, J. M., Greenhill, L. J., Diamond, P. J., Inoue, M., Nakai, N., Miyoshi, M., Henkel, C., Riess, A. 1999, 400, 6744
- Herrnstein, J. R., Moran, J. M., Greenhill, L. J., Trotter, Adam S. 2005, *ApJ*, 629, 2
- Kuo, C. Y., Braatz, J., Impellizzeri, C., Gao, F., Pesce, D., Reid, M., Condon, J., Kamali, F., Henkel, C., Greene, J. 2020, *MNRAS*, 498
- Event Horizon Telescope Collaboration et al. 2019, *MNRAS*, 875, 1
- Event Horizon Telescope Collaboration et al. 2019, *MNRAS*, 875, 1
- Event Horizon Telescope Collaboration et al. 2019, *MNRAS*, 875, 1
- Humphreys, E. M. L., Reid, M. J., Moran, J. M., Greenhill, L. J., Argon, A. L. 2013, *ApJ*, 775, 1
- Herrera-Aguilar, A., Nucamendi, U. 2015, *Phys. Rev. D*, 92
- Herrera-Aguilar, A., Nucamendi, U. 2015, *Phys. Rev. D*, 92
- Nucamendi, U., Herrera-Aguilar, A., Lizardo-Castro, R., López-Cruz, O. 2021, *ApJL*, 917
- Villalobos-Ramírez, A., Gallardo-Rivera, O., Herrera-Aguilar, A., Nucamendi, U. 2022, *Astron. Astrophys.*, 662
- Gillessen, S., Eisenhauer, F., Trippe, S., Alexander, T., Genzel, R., Martins, F., Ott, T. 2009, *ApJ*, 692, 2
- Genzel, R., Eisenhauer, F., Gillessen, S. 2010, *Rev. Mod. Phys.*, 82, 4
- Event Horizon Telescope Collaboration et al. 2022, *ApJL*, 930, 2
- Event Horizon Telescope Collaboration et al. 2022, *ApJL*, 930, 2
- Rees, Martin J. 1984, *Annu. Rev. Astron. Astrophys.*, 22
- Kormendy, J., Ho, Luis C. 2013, *Annu. Rev. Astron. Astrophys.*, 51, 1
- Riess, Adam G. et al. 1998, *Astron. J.*, 116
- Ade, P. A. R. et al. 2016, *Astron. Astrophys.*, 594
- Banerjee, P., Herrera-Aguilar, A. Momennia, M., Nucamendi, U. 2022, *Phys. Rev. D*, 105
- Pesce, D. W., Braatz, J. A., Condon, J. J., Greene, J. E. 2018, *ApJ*, 863, 2
- Villaraos, D., Herrera-Aguilar, A., Nucamendi, U., González-Juárez, G., Lizardo-Castro, R. 2022, *MNRAS*, 517
- Nucamendi, U., Herrera-Aguilar, A., Lizardo-Castro, R., López-Cruz, O. 2021, *Ap. J. Lett.*, 917, 1
- Reid, M.J., Braatz, J.A., Condon, J.J., Greenhill, L.J., Henkel, C., Lo, K.Y. 2009, *ApJ*, 695, 1
- Surcis, G., Tarchi, A., Castangia, P. 2020, *Astron. Astrophys.*, 637
- Kamali, F., Henkel, C., Brunthaler, A. et al. 2017, *Astron. Astrophys.*, 605
- Huchra, J.P., Vogeley, M.S., Geller, M. J. 1999, *ApJS*, 121, 2
- De Vaucouleurs, G., De Vaucouleurs, A., Corwin, J.H.G., Buta, R.J., Paturel, G., Fouque, P. 1991, *Third Reference Catalogue of Bright Galaxies*, Version 3.9. Springer, (New York, NY)
- Kormendy, J., Richstone, D. 1995, *Annu. Rev. Astron. Astrophys.*, 33
- Celotti, A., Miller, J. C., Sciamia, D. W. 1999, *Class. Quantum Grav.*, 16
- Schödel, R., Ott, T., Genzel, R. et al. 2002, *Nature*, 419, 6908
- Pesce D. W., Braatz J. A., Condon J. J., Gao F., Henkel C., Litzinger E., Lo K. Y., Reid M- J. 2015, *American Astron. Soc.*, 810, 1
- Rindler, W. 1982, *Introduction to special relativity* (Oxford University Press)
- Rindler, W. 1982, *Introduction to special relativity*, Oxford science publications (Clarendon Press)
- Event Horizon Telescope Collaboration et al. 2022, *Ap. J. Lett.*, 930, 2
- Villaraos, D., Herrera-Aguilar, A., and Nucamendi, U and González-Juárez, G. Lizardo-Castro, R. 2022, *MNRAS*, 517, 3
- Gravity Collaboration et al. 2020, *Astron. Astrophys.*, 636
- Gravity Collaboration et al. 2019, *Astron. Astrophys.*, 625
- Do, T., Hees, A., Ghez, A. et al. 2019, *Science*, 365, 6454
- Hees, A., Do, T., Ghez, A. M. 2017, *Phys. Rev. Lett.*, 118
- Gillessen S., Plewa P. M., Eisenhauer F., Sari R., Waisberg I., Habibi M., Pfuhl O., George E., Dexter J., Fellenberg and S. von., Ott T., Genzel R. 2017, 837, 1